

## Nickel-germanium soft x-ray zone plates

Magnus Lindblom,<sup>a)</sup> Julia Reinspach, Olov von Hofsten, Michael Bertilson, Hans M. Hertz, and Anders Holmberg

Department of Applied Physics, Biomedical and X-Ray Physics, Royal Institute of Technology, Stockholm SE-106 91, Sweden

(Received 16 January 2009; accepted 16 March 2009; published 5 May 2009)

This article presents a fabrication process for soft x-ray zone plates in which nickel and germanium are combined to achieve high diffraction efficiency. A nickel zone plate is first fabricated on a germanium film and then used as a hardmask for a  $\text{CHF}_3$ -plasma etch into the germanium. Zone plates with 50–60 nm nickel and 110–150 nm of germanium are presented. The measured diffraction efficiencies were 10%–11% at  $\lambda=2.88$  nm, which shows that high efficiency is possible even with thin nickel. Thus, the method has a potential for improving the efficiency of high-resolution zone plates for which the high-aspect-ratio structuring of nickel is difficult. © 2009 American Vacuum Society. [DOI: 10.1116/1.3117256]

The progress in nanofabrication of zone-plate optics has enabled the development of soft x-ray microscopy<sup>1</sup> into a suitable technique for nanoscale imaging in material,<sup>2,3</sup> environmental,<sup>4,5</sup> and life sciences.<sup>6–8</sup> The imaging performance is limited by the zone-plate objectives, which are circular gratings with radially increasing line density. Two properties are of special importance: the resolving power, which is determined by the outermost zone width,  $dr_N$ , and the diffraction efficiency, which depends on the optical material and its thickness.<sup>9</sup> State-of-the-art zone-plate objectives have zone widths down to about 20 nm (Ref. 10) but as small as 15 nm has been reported.<sup>11</sup> For soft x rays, electroplated nickel zone plates offer the highest efficiency and have therefore been commonly fabricated.<sup>1</sup> The smaller the zone width, the more difficult it becomes to maintain a high diffraction efficiency since the optical material must have sufficient thickness to attenuate or phase shift the x rays. The difficulty of fabricating narrow lines with high-aspect ratio (AR) therefore limits the efficiency of high-resolution zone plates.

In this article we present a fabrication process for soft x-ray zone plates in which two optical materials, nickel and germanium, are used in combination to achieve high diffraction efficiency. In this process a nickel zone plate is first fabricated on a germanium film. A nickel-germanium zone plate is then formed by using the nickel zone plate as a hardmask for a dry etch into the underlying germanium (cf. Fig. 1). The efficiency of such a zone plate, compared to a regular nickel zone plate, is shown in Fig. 2. Here the theoretical grating efficiencies at  $\lambda=2.88$  nm for different germanium thicknesses are plotted versus the nickel thickness (optically thin gratings are assumed<sup>12</sup>). The efficiency increase due to the added germanium is significant for nickel thicknesses up to about 100 nm. As typical reproducible ARs

are 4:1–5:1, a considerable improvement can be obtained for high-resolution zone plates with zone widths of about 25 nm and below.

The fabrication process is outlined in Fig. 1. Silicon nitride membranes (50 nm thick) were used as substrates and coated with a stack of materials. First, a 10 nm etch stop of Cr and then a Ge layer of the desired thickness (100–150 nm) were deposited. On top of the Ge layer a trilayer was placed, which consisted of 60 nm of ARC XL-20 (Brewer Science), a 5 nm Ti hardmask, and 25 nm of ZEP7000 (Nippon Zeon Corp.). The Cr, Ge, and Ti layers were deposited by e-beam evaporation and the plating mold material and the e-beam resist were spun cast. The only difference from our previously described process for nickel zone plates<sup>13</sup> was the thickness of the Ge layer.

The samples were patterned by e-beam lithography at 25 keV (Raith 150) and developed for 30 s in hexyl acetate. The Ti film was then structured by reactive ion etching (RIE) with  $\text{BCl}_3$  (Plasmalab 80+, Oxford Instruments) and used as a hardmask for the subsequent RIE with  $\text{O}_2$  into the polymer

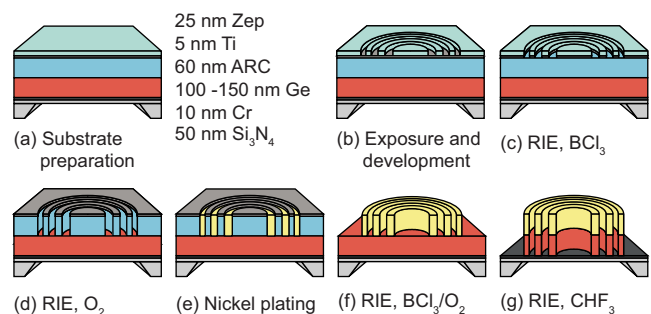


FIG. 1. (Color online) Fabrication process. A Ni zone plate is first fabricated on a Ge film [steps (a)–(f)]. The zone plate itself is then used as a hardmask for a dry etch into the Ge film [step (g)].

<sup>a)</sup>Electronic mail: magnus.lindblom@biox.kth.se

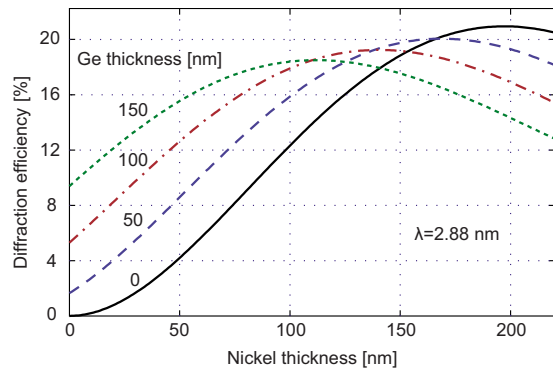


FIG. 2. (Color online) Theoretical diffraction efficiency for gratings composed of nickel and germanium. The different lines correspond to different germanium thicknesses.

plating mold material. After this, nickel was electroplated into the mold at a rate of 25–30 nm/min. To remove the Ti mask and the mold, the two RIE steps with  $\text{BCl}_3$  and  $\text{O}_2$  were repeated. At this stage in the process, the nickel zone plate is completed and the only step remaining is the pattern extension into the Ge layer.

The germanium layer was etched by RIE (Plasmalab 100, Oxford Instruments) in a  $\text{CHF}_3$  plasma with the following settings: 10 sccm (sccm denotes cubic centimeters per minute at STP) gas flow, 3 mTorr pressure, and 50 W sample power ( $0.2 \text{ W/cm}^2$ ). A helium back side pressure of 5 Torr was applied to maintain the cathode temperature at  $25^\circ\text{C}$ , but the samples were not thermally connected to the carrier wafer. The etch rate was approximately 10 nm/min which should be compared to the etch rate in nickel, 0.3 nm/min. The latter value was determined by etching into electroplated nickel films for a duration of 1 h. This resulted in an etch depth of 15–20 nm. The Ge etch with  $\text{CHF}_3$  is anisotropic, which can be seen in Fig. 3, where nickel gratings etched into a 150 nm germanium layer, are shown. The half-pitch of these gratings is 25 nm, and the nickel thickness is approximately 60 nm. Chlorine was also attempted as etch gas. It etches germanium anisotropically but forms a nonvolatile compound with the nickel that contaminates the surface. The

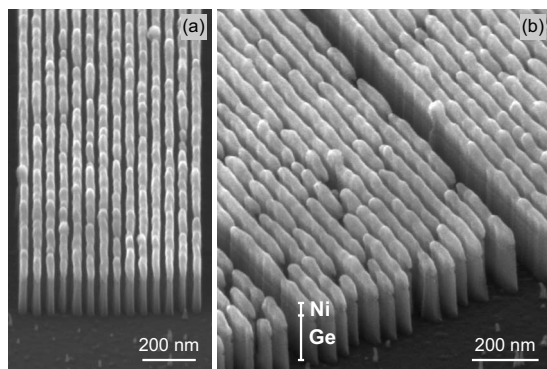


FIG. 3. Scanning electron microscopy (SEM) images of 25 nm half-pitch gratings consisting of  $\sim 60$  nm of nickel on top of 150 nm of germanium. The lines in (a) can be seen in the top right corner of the rotated view (b) ( $52^\circ$  sample tilt).

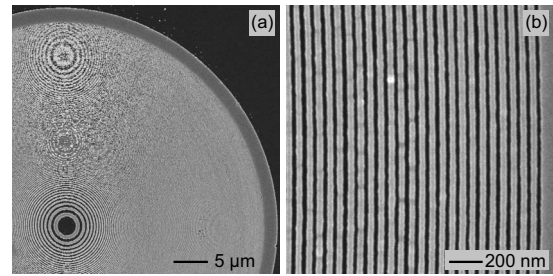


FIG. 4. SEM images of a zone plate with  $dr_N=30$  nm after the  $\text{CHF}_3$  etch. An overview (a) and a magnified view of the outer part (b).

contamination could be removed by rinsing with water but this resulted in pattern collapse for narrow lines.  $\text{CHF}_3$  is therefore preferred in this case.

To demonstrate the fabrication principle, two sets of zone plates with different germanium thicknesses are presented. One of the zone plates (with  $dr_N=30$  nm) is shown in Fig. 4. The first-order diffraction efficiency was measured at  $\lambda=2.88$  nm in a compact-source arrangement,<sup>14</sup> and the results are summarized in Table I. It is the groove efficiency that is listed which means that the substrate absorption (29%) has been compensated for. The measured efficiencies for the nickel-germanium zone plates correspond to about 70%–75% of the theoretical maximum. This is approximately the same fraction as we have previously obtained for thick nickel zone plates<sup>14</sup> ( $\sim 130$ – $150$  nm thick). Furthermore, these efficiencies are about twice as high as the theoretical maximum for nickel zone plates with the same nickel thicknesses as the nickel-germanium zone plates had before the germanium etch (cf. Table I).

The amount of nickel lost in the  $\text{CHF}_3$ -plasma etch was calculated from the measured nickel etch rate of 0.3 nm/min. The etch time used was 15 min for 115 nm of germanium and 25 min for 150 nm of germanium, which gives nickel losses of 5 and 7.5 nm, respectively. The film thickness measurements were carried out with profilometer scans (Tencor

TABLE I. Zone-plate parameters and measured efficiencies.  $dr_N$  is the width of the outermost zone,  $t_{\text{Ni}}$  is the plated nickel thickness before the Ge etch,  $t_{\text{Ge}}$  is the thickness of the Ge film,  $\eta$  is the measured groove efficiency, and  $\eta_{\text{Ni}}$  is the maximum theoretical efficiency for a nickel zone plate with a thickness equal to  $t_{\text{Ni}}$ .

$dr_N$ (nm)	$t_{\text{Ni}}$ (nm)	$t_{\text{Ge}}$ (nm)	$\eta$ (%)	
			Expt.	Theor.
50	62	115	10.9	6.0
50	50	115	10.6	4.2
50	59	115	10.3	5.6
50	61	115	10.9	5.9
50	58	115	10.7	5.4
30	57	150	11.1	5.1
30	58	150	10.9	5.3
30	58	150	10.7	5.3
25	56	150	10.3	5.0

P-15). While the germanium thickness can be accurately measured after the vapor deposition, it is difficult to measure the thickness of thin electroplated nickel films since the electroplating process produces local thickness variations and grains with sizes of the order of 10–20 nm (cf. Fig. 3). However, since the mold thickness is accurately known and the profilometer tip scans on top of the grains (the tip has a 2  $\mu\text{m}$  radius of curvature), the nickel thickness is not underestimated. This is important as an underestimation of the nickel thickness would result in a corresponding overestimation of the efficiency increase due to the added germanium.

In summary, we have presented a fabrication process for soft x-ray zone plates composed of nickel and germanium and showed that such zone plates can attain high diffraction efficiency even with thin nickel. We therefore conclude that the technique can be useful for the fabrication of high-resolution zone plates with high diffraction efficiency. Alternatively, it can be used to avoid electroplating high ARs in order to improve process yield. We also believe that this fabrication concept is not limited to this particular material combination or to soft x-ray optics. It should be applicable to other combinations of optical materials as well, given that one of them can serve as etch mask.

The authors gratefully acknowledge the financial support of the Swedish Science Research Council, the Swedish Foundation for Strategic Research, the Wallenberg Foundation, and the Göran Gustafsson Foundation.

- <sup>1</sup>S. Aoki, Y. Kagoshima, and Y. Suzuki, *X-Ray Microscopy* (IPAP, Tokyo, Japan, 2006).
- <sup>2</sup>B. van Waeyenberge *et al.*, *Nature* (London) **444**, 461 (2006).
- <sup>3</sup>P. Fischer, *IEEE Trans. Magn.* **44**, 1900 (2008).
- <sup>4</sup>S. C. B. Myneni, J. T. Brown, G. A. Martinez, and W. Meyer-Ilse, *Science* **286**, 1335 (1999).
- <sup>5</sup>J. Thieme, S. C. Gleber, P. Guttman, J. Prietzel, I. McNulty, and J. Coates, *Miner. Mag.* **72**, 211 (2008).
- <sup>6</sup>J. Kirz, C. Jacobsen, and M. Howells, *Q. Rev. Biophys.* **28**, 33 (1995).
- <sup>7</sup>D. Y. Parkinson, G. McDermott, L. D. Etkin, M. A. Le Gros, and C. A. Larabell, *J. Struct. Biol.* **162**, 380 (2008).
- <sup>8</sup>W. Meyer-Ilse, D. Hamamoto, A. Nair, S. A. Lelievre, G. Denbeaux, L. Johnson, A. L. Pearson, D. Yager, M. A. Legros, and C. A. Larabell, *J. Microsc.* **201**, 395 (2001).
- <sup>9</sup>A. G. Michette, *Optical Systems for Soft X-Rays* (Plenum, New York, 1986).
- <sup>10</sup>M. Peuker, *Appl. Phys. Lett.* **78**, 2208 (2001).
- <sup>11</sup>W. Chao, B. D. Harteneck, J. A. Liddle, E. H. Anderson, and D. T. Attwood, *Nature* (London) **435**, 1210 (2005).
- <sup>12</sup>J. Kirz, *J. Opt. Soc. Am.* **64**, 301 (1974).
- <sup>13</sup>A. Holmberg, S. Rehbein, and H. M. Hertz, *Microelectron. Eng.* **73–74**, 639 (2004).
- <sup>14</sup>M. Bertilson, P. A. C. Takman, U. Vogt, A. Holmberg, and H. M. Hertz, *Rev. Sci. Instrum.* **78**, 026103 (2007).